Proceedings World Geothermal Congress 2020+1
Reykjavik, Iceland, April - October 2021

Tensile Testing of Casing Material at Elevated Temperatures up to 550°C

Bert Dillingh[1], Gunnar Skúlason Kaldal[2], Ingólfur Thorbjornsson[2], Jens Wollenweber[1], Frank Vercauteren[1]

[1]TNO – Dutch Organization for Applied Research – The Netherlands

[2]ISOR – Iceland GeoSurvey, Grensásvegi 9, 108 Reykjavík, Iceland

bert.dillingh@tno.nl

Keywords: tensile testing, thermal stress, elevated temperature, material properties, casing

ABSTRACT

In high-temperature geothermal wells the casing is subjected to tremendous stresses and strains, particularly at temperatures above 200°C. When anchored to the formation or an external casing by cement, stress in the casing can easily exceed the yield stress locally. The associated plastic strain cycles during several well discharges can be such that the casing material properties deteriorates quickly and can lead to casing failure. Casing material data at such temperatures is not readily available for typical casing material candidates used for geothermal wells. Therefore, tensile tests were performed at room temperature, elevated (250°C) and high temperatures (450°C, 550°C) for the proposed material candidates (K55, L80, T95 and nickel-chromium alloy Inconel 625). The test series was conducted in the GeoWell project that was funded under the EU Horizon 2020 framework. Significant strength reductions with increasing temperature were observed. The test series results are in good agreement with design curves that are given up to 350°C in the New Zealand standard (NZS 2403:2015) with respect to the yield and tensile multiplication factors.

1. INTRODUCTION

In a geothermal well the casing is subjected to tremendous cyclic stresses and strains, particularly at temperatures above 200°C. When anchored to the formation by cement, the casing can easily exceed the yield stress locally. The associated plastic strain cycles during several well discharges can be such that the casing material properties deteriorates quickly and can lead to early casing failure.

To meet well integrity requirements required for safe and prolonged (high-temperature) geothermal operations, several solutions are proposed in the GeoWell project to lower the casing stresses and strains. One of the proposed solutions is the design of an axial compensator, i.e. a flexible coupling (Thorbjörnsson & Kaldal, 2020). Though the design is intended to eliminate most axial stresses, there will still be locations left with high stresses. At elevated temperatures, e.g. exceeding 450°C (Ingason et al., 2014) in the IDDP-1 well of the Icelandic Deep Drilling Project, the casing's mechanical properties are compromised (Kaldal et al., 2016).

Material data at such temperatures is not readily available for typical casing material candidates. ÍSOR provided samples of selected casing materials (K55, L80, T95 and Inconel 625). Tensile tests were performed at TNO's Structural Dynamics Lab at room temperature, elevated (250°C) and high temperatures (450°C, 550°C) for the proposed material candidates.

2. TEST SET-UP AND TEST PROCEDURE

The tests are performed in a MTS tensile rig with a capacity of 250 kN, see Figure 1. To enable high temperature testing the rig is equipped with an oven capable of reaching temperatures of 1200°C.

Figure 1: MTS tensile rig with integrated oven.

The experiments are conducted in accordance to the standard ASTM E8M (Test Methods for Tension Testing of Metallic Materials) and ASTM E21 (Practice for Elevated Temperature Tension Tests of Metallic Materials). The load-measuring system is in accordance with ASTM E4 & E74, the extensometers are in accordance with ASTM E83 and the thermocouples are in accordance with ASTM E220.

For measuring the strain at high temperatures special high temperature Linear Variable Displacement Transducer (LVDT) are used, see Figure 2. The LVDT's are designed with the active measurement element outside the oven. The HT-LVDT design is such that the strain measurement is insensitive to temperature changes over a large temperature range. To be able to use these HT-LVDT's the tensile specimens require collars to fit the HT-LVDT's clamps. In Figure 3 the tensile specimen's geometry is given. The sample's temperature of the specimen is actively monitored using a type E thermocouple. The thermocouple's tip is shielded from direct radiation for accurate determination of the temperature, see Figure 4.

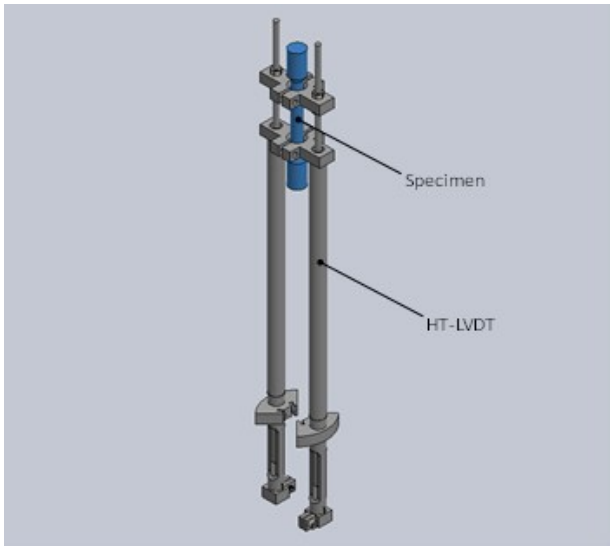

Figure 2: High Temperature LVDT used in the experiments.

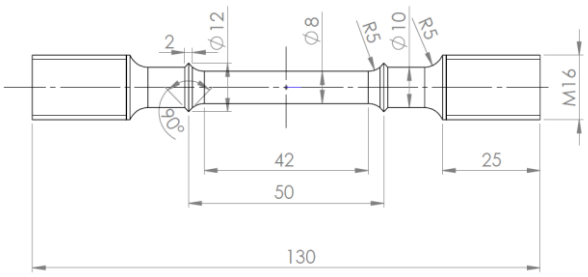

Figure 3: Tensile specimen's geometry specifications.

Figure 4: Actual temperature measurement of the sample during the experiment with type E thermocouple.

3. MATERIAL PROPERTIES

In the selection process of potential material candidates, a long list of materials was proposed, see Table 1. The rationale for this list is incorporation of materials already used in casing design and add several new materials that could fulfill the requirement of high temperature application.

Table 1: Casing material candidates.

Material Candidate	Material Description
K55	Carbon Steel
L80	Carbon Steel
T95	Carbon Steel
API X65	Carbon Steel
254SMO (AISI S31254)	Austenitic Stainless Steel
654SMO	Austenitic Stainless Steel
NO-6625 (Inconel 625)	Nickel Base Material
Titanium grade9	Titanium Base Material
WN 1.4724	Ferritic Stainless Steel
WN 1.4742 (Therma4742)	Ferritic Stainless Steel
WN 1.4762	Ferritic Stainless Steel
253MA (WN1.4835)	Micro Alloyed Austenitic Stainless Steel

The materials were assessed in terms of the following criteria: Stress Corrosion Cracking (SCC) resistance, chlorides resistance, corrosion resistance, weldability, material strength & ductility, Coefficient of Thermal Expansion (CTE), Cost, availability, etc. The wide variety of requirements for the harsh conditions in a geothermal well reduced the number of materials considerably. The final chosen set of materials are K55, L80, T95 and Inconel 625. The K55, L80 and T95 were all provided in a Quenched and Tempered (QT) condition. The provided material comprises coupons of tube walls and varied between 8 and 15 mm. Therefore, the tensile specimens required the full thickness of the provided tube wall material. All specimens can be assumed to be 1/2T type specimens and were taken in the tube's axial direction.

4. RESULTS

In this chapter an overview will be given for the combined results per material. If there are any deviations, they will be discussed.

4.1 Overview results K55 material

In Figure 5 the combined results of the K55 material are presented. The results up to the Ultimate Tensile Stress (UTS) at every temperature reproduce very well between the experiments. The most noticeable difference is found in the tests at 450°C.

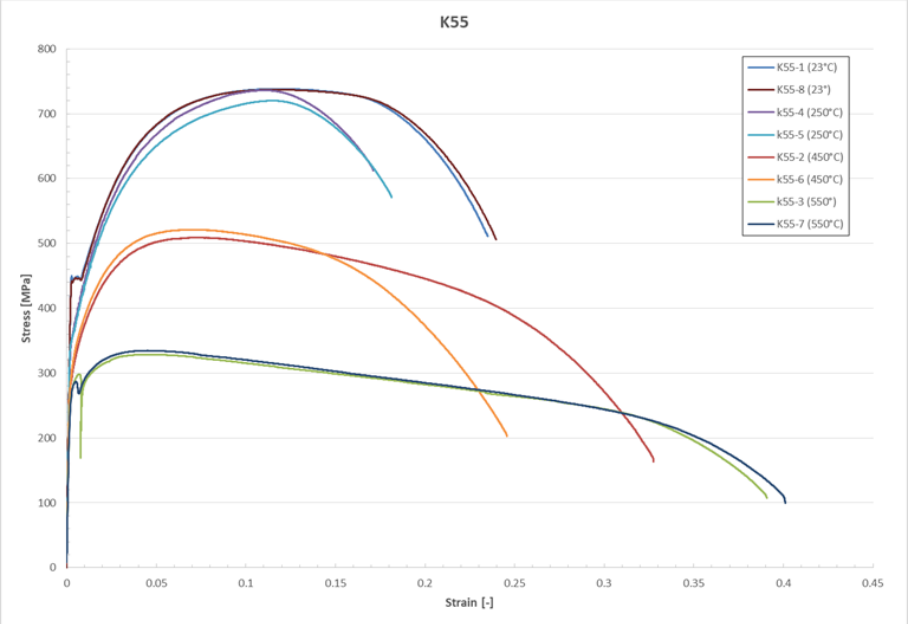

Figure 5: Tensile test results for K55 at various temperatures.

Comparing the fracture surfaces and necking profiles see Figure 6, the necking of the K55-6 seem a bit more localized. This explains the smaller failure strain and lesser amount of absorbed energy. Though the size of the ductile core area versus the shear

lip area seems quite comparable. This means the actual fracturing process was not so much affected by the overall necking profile (i.e. the amount of tri-axial state of stress). Though it seems one of the experiments could be an outlier, it seems more probable that this spread is a regular spread in the results at this particular temperature which is apparently very sensitive to the value of the UTS and uniform strain value.

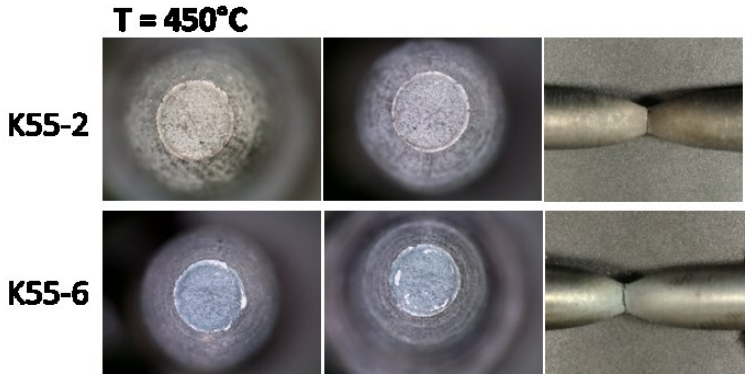

Figure 6: Fracture surfaces and necking profile for experiments K55-2 and K55-6 both tested at 450°C.

At room temperature and at the yield stress the characteristic yielding plateau common for low carbon steels is present when the Lüders bands form. At higher temperatures they tend to disappear as can been seen at 250°C and 450°C. Though at 550°C it re-appears once as a dip just beyond the yield point. In experiment K55-3 the dip is very deep. This is not believed to be the actual decrease but merely an artefact of the control system handling the quick changes in the specimens response. The results of K55-7 give a more gradual and more likely actual response around the yield dip.

4.2 Results L80 material

In Figure 7 the overview of all tensile test at the L80 materials are presented. This material is very predictable in its behavior. The values for yield stress and UTS drop consistently at higher temperature and the failure strain increases with an increase in temperature. The spread in failure strain also increase with a rise in temperature.

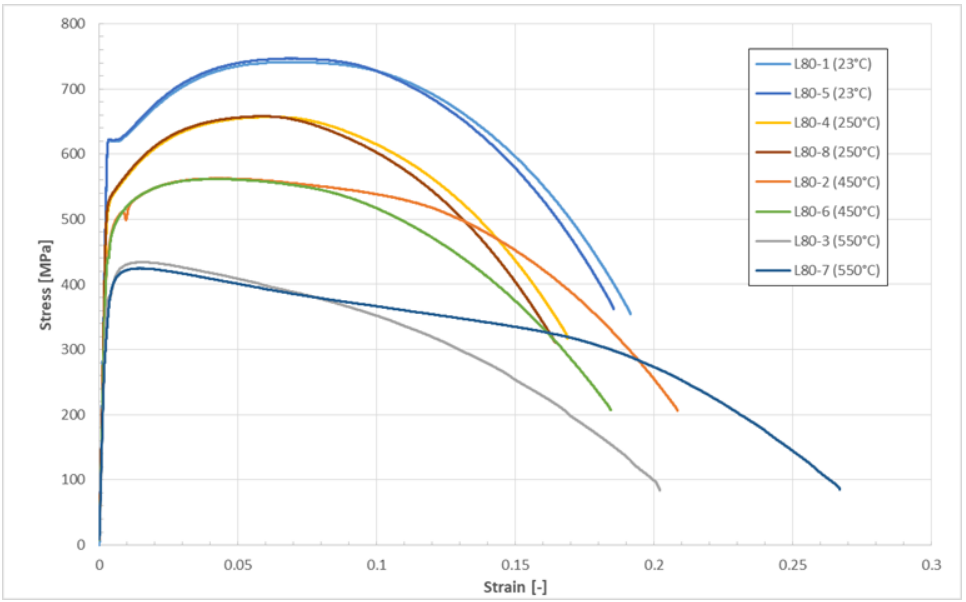

Figure 7: Tensile test results for L80 at various temperatures.

4.3 results T95 material

In Figure 8 the overview of all tensile tests at the T95 materials are presented. The T95 is very predictable in its behavior as well. The values for yield stress and UTS drop consistently at higher temperature. Most remarkable about this material is the rather constant failure strain over all temperatures.

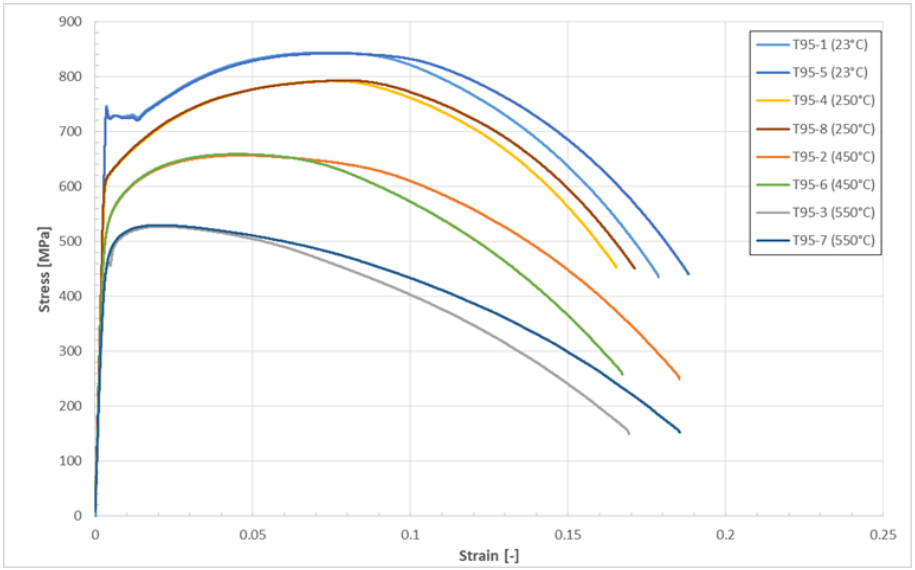

Figure 8: Tensile test results for T95 at various temperatures.

Results Inconel 625

In Figure 9 the overview of all tensile test at the Inconel 625 materials are presented. As can be seen in the graph, the curves at room temperature are very smooth while at all the higher temperatures the situation is quite different and looks noisy. This seemingly disturbed signal is actually coming from the deforming material itself. During the tensile test the plastic deformation is actually audible. A sound can be heard, sounding like clicks or ringing noises. The pitch of these noises varies with temperature. What is occurring in the Inconel is often referred to as Dynamic Strain Aging (DSA) or it is also known as the Portevin–Le Chatelier effect (or PLC effect) see e.g. Maj (2017) and Grzegorczyk (2013).

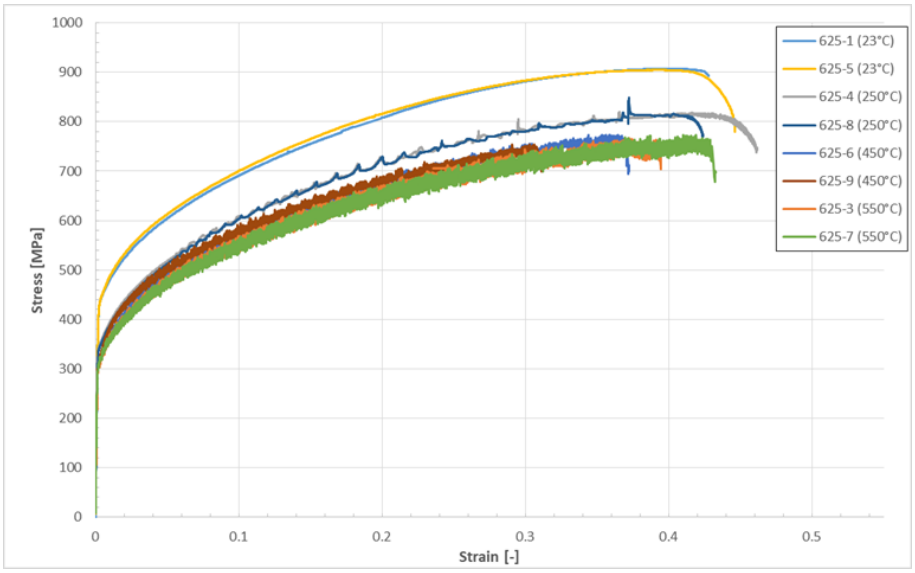

Figure 9: Tensile test results for Inconel 625 at various temperatures.

Portevin – Le Chatelier Effect

Some materials are prone to this effect and manifest themselves at particular temperatures and strain rates ranges. The PLC effect is caused by the diffusion of solute atoms towards mobile dislocations (caused by the plastic deformation). Dislocations block the progress of the mobile dislocations and causes the material to harden. While the external stress is still increasing, the blockade is breached at some point and the dislocations can continue their "journey" but they now run into areas which are now diluted from their solutes. This diluted zone translates into a less resistant material for a short time until the dislocation get stuck again somewhere and the solutes have time to reach this new location and the process repeats.

Because temperature is the most important driver for the diffusion rate of the solutes, these solutes reach their destination faster at higher temperatures and hence the material finds itself less time in a 'weaker' region. Faster response of the solutes at higher temperature translate to a higher pitch in the stress-strain curve.

The other important factor is the plastic strain rate. This plastic strain rate determines the speed of dislocations through the material. If the dislocation velocity is much higher than the diffusion of the solutes (which is the case at lower temperatures), the dislocations run through the matrix which is hampered by a given concentration of inclusions and an average concentration of solutes, given rise to a smooth plastic deformation. On the other hand if temperature and/or plastic strain rate changes, the balance can be such that oscillations in material resistance develop and the stress-strain curve becomes serrated. When the PLC effect is active, often crosses at the surface are visible, see Figure 1Figure 10. These features are caused by discrete shear lines that occur in the material. These lines extend up to the surface where they are clearly visible.

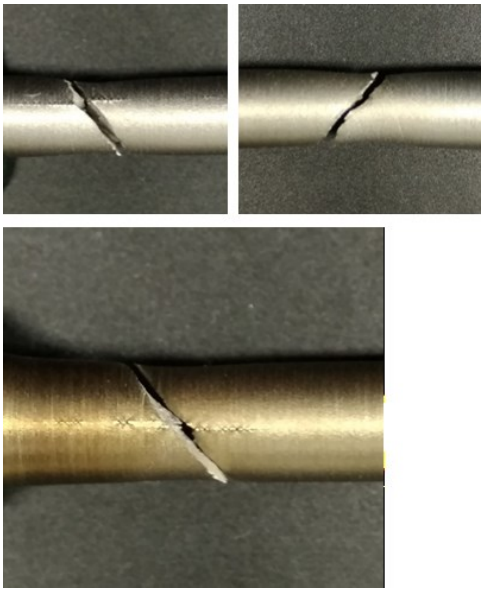

Figure 10: typical fracture for Inconel625 when the PLC effect is active. Also note the crosses at the surface causes by discrete shear lines in the material.

In Maj (2017) several classes or regimes for the ratio between temperature and plastic strain rate are identified. These translate to some kind of fingerprint in the oscillating patterns. Looking at the patterns the specific combination of temperature and plastic strain rate were active can be derived.

If the material Inconel625 is used in an application wherein a low cycle fatigue loading could exist, it is recommended to test for this condition as well because the PLC effect could be detrimental in that case. It is furthermore important to understand that long term aging effects become important when the geothermal well is in use over prolonged periods of time. Long-term aging in steels at high temperatures is a very complex process and is outside the scope of this study, but one should be aware that these microstructural changes do have an effect on the mechanical properties over time. Also, at the highest reported temperatures creep phenomena can start to play a role in the mechanical behavior as well.

4.5 Summary of results

In Table 2,3,4 and 5 the summary of mechanical properties is given for K55, L80, T95 and Inconel625 respectively.

Table 2: Summary mechanical properties K55 for various temperatures.

Sample	Temp [°]	σ0.2 [MPa]	UTS [MPa]	εu [-]	σf [-]	Yield factor	UTS factor
K55-1	23	443.3	738.2	0.235	512.0	1.00	1.00
K55-8	23	444.0	737.1	0.240	506.5	1.00	1.00
K55average	23	443.7	737.7	0.238	509.25	1.00	1.00
K55-4	250	366.0	736.0	0.171	612.2	0.83	1.00
K55-5	250	361.1	720.2	0.181	570.8	0.81	0.98
K55average	250	363.6	728.1	0.176	591.5	0.82	0.99
K55-2	450	271.9	509.0	0.328	163.8	0.61	0.69
K55-6	450	319.7	521.2	0.246	202.4	0.72	0.71
K55average	450	295.8	515.1	0.287	183.1	0.67	0.70
K55-3	550	280.7	328.7	0.408	107.4	0.63	0.45
K55-7	550	280.5	334.7	0.401	99.4	0.63	0.45
K55average	550	280.6	331.7	0.405	103.4	0.63	0.45

Table 3: Summary mechanical properties L80 for various temperatures.

Sample	Temp [°]	σ0.2 [MPa]	UTS [MPa]	εu [-]	σf [-]	Yield factor	UTS factor
L80-1	23	619.7	741.1	0.192	354.5	1.00	1.00
L80-5	23	621.4	746.6	0.185	362.1	1.00	1.01
L80average	23	620.6	743.9	0.189	358.3	1.00	1.00
L80-4	250	534.6	656.9	0.169	316.7	0.86	0.89
L80-8	250	536.8	657.9	0.164	309.9	0.87	0.89
L80average	250	535.7	657.4	0.167	313.3	0.86	0.89
L80-2	450	481.3	562.6	0.208	206.1	0.78	0.76
L80-6	450	473.0	561.9	0.184	207.0	0.76	0.76
L80average	450	477.2	562.3	0.196	206.6	0.77	0.76
L80-3	550	392.1	434.1	0.202	83.3	0.63	0.59
L80-7	550	388.2	424.6	0.267	85.7	0.63	0.57
L80average	550	390.2	429.4	0.235	84.5	0.63	0.58

Table 4: Summary mechanical properties T95 for various temperatures.

Sample	Temp [°]	σ0.2 [MPa]	UTS [MPa]	εu [-]	σf [-]	Yield factor	UTS factor
T95-1	23	726.0	843.8	0.179	435.5	1.00	1.00
T95-5	23	726.2	842.2	0.188	439.9	1.00	1.00
T95average	23	726.1	843	0.184	437.7	1.00	1.00
T95-4	250	625.4	792.2	0.165	452.2	0.86	0.94
T95-8	250	624.4	793.0	0.171	450.1	0.86	0.94
T95average	250	624.9	792.6	0.168	451.15	0.86	0.94
T95-2	450	543.2	656.7	0.185	249.2	0.75	0.78
T95-6	450	543.6	658.9	0.167	258.0	0.75	0.78
T95average	450	543.4	657.8	0.176	253.6	0.75	0.78
T95-3	550	456.7	526.6	0.169	148.8	0.63	0.62
T95-7	550	480.7	529.6	0.185	152.2	0.66	0.63
T95average	550	468.7	528.1	0.177	150.5	0.65	0.63

Table 5: Summary mechanical properties Inconel 625 for various temperatures.

Sample	Temp [°]	σ0.2 [MPa]	UTS [MPa]	εu [-]	σf [-]	Yield factor	UTS factor
625-1	23	444.3	906.9	0.428	892.3	1.00	1.00
625-5	23	443.6	904.8	0.447	781.1	1.00	1.00
625average	23	444.0	905.9	0.438	836.7	1.00	1.00
625-4	250	352.2	820.1	0.462	742.1	0.79	0.90
625-8	250	350.7	848.3	0.424	769.7	0.79	0.94
625average	250	351.5	834.2	0.443	755.9	0.79	0.92
625-6	450	322.3	773.7	0.372	693.5	0.73	0.85
625-9	450	326.7	753.8	0.311	698.9	0.74	0.83
625average	450	324.5	763.8	0.342	696.2	0.73	0.84
625-3	550	313.1	766.1	0.395	731.1	0.70	0.84
625-7	550	324.5	773.6	0.433	698.0	0.73	0.85
625average	550	318.8	769.9	0.414	714.6	0.72	0.85

5. DISCUSSION

Overall the materials K55, L80, T95 and Inconel625 behave in an expected manner in a sense that with increasing temperature the yield and ultimate tensile stress drop consistently as well as the uniform strain (though there is exception for K55). A pattern for the failure strain is more complicated. Normally it would increase for increasing temperature but that is not the case all the time. Material instability at the UTS causes variances in the remainder of the stress-strain curve (i.e. between the uniform strain and failure strain). Because of the instable character and regular small differences in geometry and testing variations, the variation between experiments is most noticeable in this last part of the stress-strain curve. This is the main reason for variances in the failure strain. Any found differences in failure strain under a given condition could not be correlated with any differences in the fracture surface. The ratio between the core 'cup' and the shear lips (i.e. the cone) were found to be almost identical. So the variance in failure strain can be considered a natural variance in the results.

The only material that significantly differs from the other three materials is Inconel625. Uniform strains and failure strains outperforms the other materials on each temperature tested. Though the yield stress is not that impressive compared to the other materials, its stability over a large temperature range, again outperforms the other materials. The same consistent behavior applies to the UTS over the tested temperature range.

Finally, the observed serrated stress-strain behavior at higher temperature and low strain rates, is explained by Dynamic Strain Aging or the PLC effect. Though the material's constitutive behavior under monotonously increasing load is very good, its behavior under low cycle fatigue is less known and needs to be tested separately.

In general at the highest reported temperatures, long term aging effects can have both detrimental or beneficial consequences. Long term aging effects in steels at high temperatures are very complex and outside the scope of this study, though it is certain the highest temperatures will affect the mechanical properties in the long run. Another aspect that becomes of importance at these temperatures is creep. Though creep is normally associated with even higher temperatures, possible high stresses arising from strain constraints can certainly place the material in the creep regime.

Discussion on the comparison with the New Zealand standard

The New Zealand standard on deep geothermal wells has a paragraph on casing properties and performance properties, see paragraph 2.9 of NZS 2403:2015.

In Figures 11-14 and in Table 6 a comparison is made between the results obtained by the NZS and the results of this study. Overall the comparison at 250°C (i.e. this temperature is actually the only temperature that can be compared) the results are in good agreement. The presented yield stress is a bit lower than the NZS series but only to a small degree and is within the 5% margin which stated by the NZS as a normal deviation. At the tensile strength the presented results are bit higher. This can easily be the case because the NZS present a lower bound value in the table. For higher temperatures (450 and 550°C) no comparison can be made, the only observation is that the TNO/GeoWell test series results are in line with an expected continuously decreasing yield and strength factor at increasing temperatures.

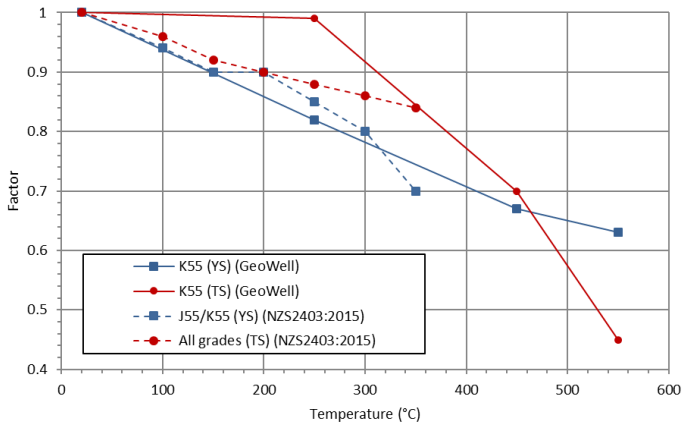

Figure 11: Reduction factors for yield and tensile stress for the K55 material.

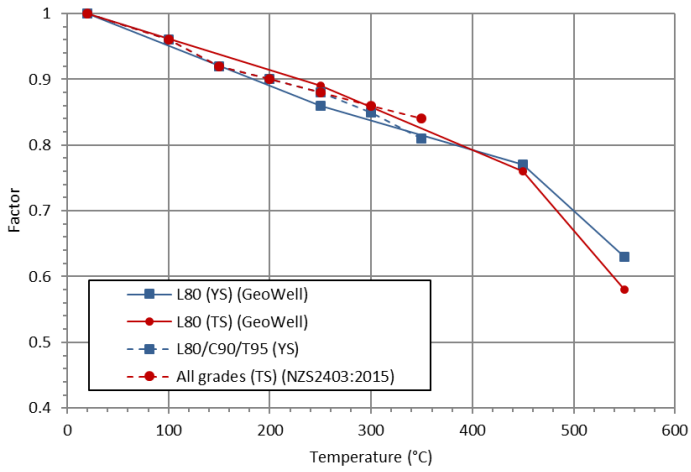

Figure 12: Reduction factors for yield and tensile stress for the L80 material.

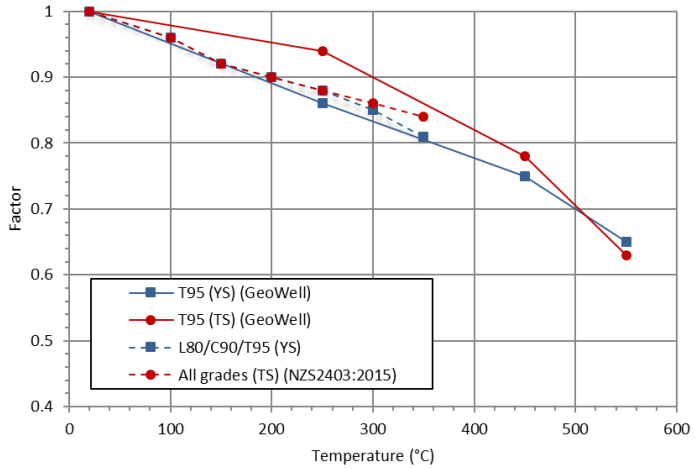

Figure 13: Reduction factors for yield and tensile stress for the T95 material.

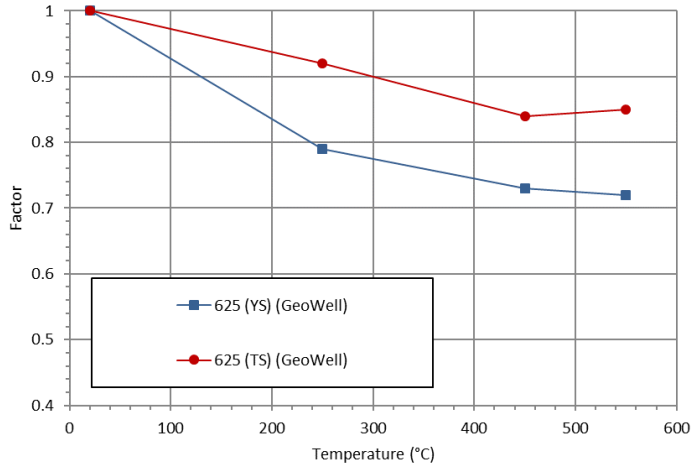

Figure 14: Reduction factors for yield and tensile stress for the Inconel 625.

Table 6: Overview and comparison of the yield and strength factors from the NZS and TNO/GeoWell experiments.

	Temperature [°C]								
	20/23*	100	150	200	250	300	350	450**	550**
Grade	**API yield strength (factor)**								
J55/K55 by NZS	1.00	0.94	0.90	0.90	0.85	0.80	0.70		
J55/K55 by Geowell	1.00				0.82			0.67	0.63
L80/C90/T95 by NZS	1.00	0.96	0.92	0.90	0.88	0.85	0.81		
L80/T95 by Geowell	1.00				0.86			0.76	0.64
Inconel625 by Geowell	1.00				0.79			0.73	0.72
	Tensile Strength (factor)								
All grades by NZS	1.00	0.96	0.92	0.90	0.88	0.86	0.84		
K55/L80/T95 by Geowell	1.00				0.94			0.75	0.55
Inconel625 by Geowell	1.00				0.92			0.84	0.85

*there a slight difference in room temperature between the NZS and TNO/GeoWell test series. The difference is small and is expected to be of minor importance.
**The temperature 450 and 550°C were only measured in the TNO/GeoWell test series, while 100, 150, 200, 300 and 350 were given in the NZS series.

The NZS standard states that the selected materials should be selected from API Spec 5CT or API Spec 5L. Though especially in corrosive environments the standard allows for other options. In case of the presence of gases, the dangers of Hydrogen Embrittlement and Sulphide Stress Corrosion on the materials should be addressed. Such materials should apply to the standard ANSI/NACE MR 0175/ISO 15156 for approval. The use materials K55, L80, T95 already qualified according to this standard. Establishing Inconel625 corrosive properties is outside the scope of this investigation but was explored in GeoWell by Thorbjornsson et al. (2020). If new materials are introduced the standards also prescribes long term testing of the material. According to the NZS it is also allowed to use liners as a corrosive barrier or even fiber reinforced materials may be used.

6. CONCLUSIONS

The engineering stress-strain curves have been established for four casing materials K55, L80, T95 and Inconel625 at various temperatures (i.e. 23, 250, 450 and 550°C). The presented test series results are in good agreement with and extend the data from the New Zealand Standard (NZS) with respect to the yield and tensile multiplication factors. The test results are within the required limits.

Serrated yielding was found for Inconel625 for all temperatures except at room temperature and at the prescribed low strain rate. The serrated yielding can be explained by the PLC-effect.

7. ACKNOWLEDGMENTS

This GeoWell project has received funding from the European Union's Horizon 2020 research and innovation program under grant agreement No 654497. We also would like to thank our partners from ISOR: Gunnar Skúlason Kaldal, Árni Ragnarsson, Ingólfur Örn Þorbjörnsson for their support and advice in the material candidate selection process.

REFERENCES

Maj, P., Zdunek, J., Mizera, J., Kurzydlowski, K., Sakowicz, B. and Kaminski M.: Microstructure and Strain-Stress Analysis of the Dynamic Strain Aging in Inconel 625 at High Temperature, Met. Mater. Int., **23**, No. 1, 54-67 (2017).

Grzegorczyk, B., Ozgowicz, W., Kalinowska-Ozgowicz, E., Kowalski, A.: Investigation of the Portevin-Le Chatelier effect by the acoustic emission, Journal of Achievement in Materials and Manufacturing Engineering, **60**, No.1, 7-14 (2013)

Ingason, K., Kristjánsson, V., Einarsson, K., 2014. Design and development of the discharge system of IDDP-1. Geothermics 49, 58-65.

Kaldal, G. S., Jónson, M. T., Pálsson, H. & Karlsdóttir, S. N., 2016. Structural modeling of the casings in the IDDP-1 well: Load history analysis. Geothermics, pp. 1-11.

Thorbjörnsson, I. & Kaldal, G. S., 2020. Flexible Couplings for Improved Casing Design in high-temperature Geothermal Wells (in proceedings). Reykjavík, World Geothermal Congress.

Thorbjornsson, I.O., Krogh, B.C., Kaldal, G.S., Rørvik, G., Jonsson, S., Gudmundsson L., Oskarsson, F., Sigurdsson, O., Husby, H., Ragnarsson, A., 2020. Corrosion Testing in Direct Geothermal Steam of Cladded and Standalone Materials at 210 °C and 450 °C (in proceedings). Reykjavík, World Geothermal Congress.

NZS 2403:2015, 2015. NZS 2403:2015 Code of practice for deep geothermal wells. Standards New Zealand, Private Bag 2439, Wellington 6140 (2015).